Influence of Metal and Nonmetal Ion Doping on the Photocatalytic Performance of Iron Oxide Nanoparticles

Baraa A. Kareem
Ban M. Alshabander

Department of Physics, College of Science, University of Baghdad, Baghdad, IRAQ

In this research, iron oxide (Fe_2O_3) nanoparticles were doped with 5% mol of metallic materials (Ag, Co, Cu) and non-metallic materials (S, N), and they were prepared by a simple impregnation method. The morphological features and elemental composition of the Fe_2O_3 nanoparticles were introduced. Moreover, nanoparticles of the photocatalytic activities of Fe_2O_3 with Ag, Co, Cu, S and N nanocomposites were examined by methyl blue solution as a model of pollutant. This study showed that Fe_2O_3/Ag, Co, Cu, S, and N nanoparticles possess good degradation of MB solution, reaching 80%, 51%, 48%, 45%, 68%, and 33% after 240 minutes of UV light. As can be seen, Ag is the better photocatalyst since adding silver as a dopant strongly reduces the recombination onto the photocatalyst surface, increasing the lifetime of electrons and holes and thus releasing more hydroxyl radicals.

Keywords: Degradation; Nanoparticles; Magnetite; Photocatalysts
Received: 14 July 2024; Revised: 29 September; Accepted: 06 October 2024

1. Introduction

The pollution of water has become a critical problem over the modern decades [1]. Water contamination is one of the main reasons for the infliction of ecological imbalance. The rapid growth in dye manufacturing, ink, paper, food processing, and textiles exacerbated this situation. Wastes from these industries, dumped into nearby water bodies, may contain large amounts of toxic, non-biodegradable, and complex molecular structure dyes [2]. Among such dyes are some that have characteristics that show extremely drastic effects on aquatic and terrestrial life. There are multiple techniques available for purifying water, such as heat treatment, filtration [3], chemical absorption, and biological processes. The generated hydroxyl radials and super oxygen species are considered effective methods for treating water pollutants with the help of heterogeneous photocatalytic oxidation. Much effort has been made to doping metals and nonmetals to enhance their photocatalytic activity. Hence, nanoparticles have widely been used as catalysts in overwhelmingly large reactions [4]. In a photocatalytic context, semiconductor nanoparticles like Fe_2O_3, ZnO, and TiO_2 have been used to carry out light-induced transformations [5,6]. Iron trioxide is a compound consisting of iron and oxygen and is mostly utilized for numerous fields of applications like biotechnology [7], catalyst [8], lithium-ion battery [9], environmental remediation [10], magnetic fluid [11] and magnetic resonance imaging [12]. The Fe_2O_3 photocatalyst has attracted much attention due to its low cost, high stability [13], nontoxicity [14], excellent anti-ferromagnetic characteristics [15], and environmentally friendly properties with a band gap of ca. 2.2-2.3 eV. Fe_2O_3 can be synthesized using several methods, such as the hydrothermal approach [16-17], sol-gel [18-19], impregnation method [20], and precipitation method [21-22] Polyol synthesis [23-24]. These techniques can also be utilized to make other metal oxides with metallic (Ag, Cu, Co) and non-metallic (N, S) components. Dopants, whether metallic or non-metallic, can enhance the photocatalytic efficiency of Fe_2O_3 photocatalysts by prolonging the lifespan of carriers and broadening the range of light absorption. We tested the nanocomposite materials made through photocatalytic degradation using MB (Methylene Blue) dyes to see how well they worked.

The aim of this work is to prepare iron composites Fe_2O_3/Ag, Co, Cu and Fe_2O_3/N, S by impregnation method and studying the effect of these metallic and non-metallic materials on the effectiveness of photocatalysis when exposed to sunlight for different periods of time.

2. Experimental Part

Iron oxide (Fe_2O_3), silver nitrate ($AgNO_3$), cobalt chloride hexahydrate ($CoCl_2.6H_2O$) and copper nitrate ($CuNO_3.3H_2O$) were used as sources of Ag, Co, and Cu to prepare Fe_2O_3/metal nanocomposites. Urea (CH_4N_2O) and sodium sulfide (Na_2SO_4) are the sources of N and S to prepare Fe_2O_3/nonmetal nanocomposites. The raw materials were purchased from Sigma-Aldrich, and Fe_2O_3 was purchased from Sky Spring Nanomaterials with particle size 20-40nm. The azo dye, methyl blue ($C_{16}H_{18}CIN_3S$) (MB) was supplied from Sigma-Aldrich.

The preparation of samples was achieved by adding 5% moles of Cu, Co, Ag, N, or S to 1 g of Fe_2O_3 powder. Additionally, 20 mL of distilled water are added to the mixture of Fe_2O_3/metal and Fe_2O_3/nonmetal. The solution was thoroughly mixed with distilled water under agitation using magnetic stirrers at a temperature of 90 °C and a speed of 1500 rpm for 60 minutes to achieve a well-homogenized

solution. Afterward, it was subjected to two washes with distilled water to remove any potential impurities or contaminants. Subsequently, the sample was dried at a temperature of 110 °C in an oven. As a result, both the Fe_2O_3/metallic and Fe_2O_3/non-metallic nanocomposites will exhibit a brown color. Finally, it is crushed into a fine powder using an agate mortar.

The surface morphology was identified by JEOL-JSM-6360 (Japan) scanning electron microscope (SEM) operated at 20kV and equipped with an energy-dispersive x-ray spectroscopy (EDX) system. The FTIR spectra were recorded using a Shimadzu 8400S (Japan) instrument from 4000 to 400 cm^{-1} by KBr pallet method. A Shimadzu 3600 NIR (Japan) instrument was used for measuring UV-visible absorption spectra.

Photocatalytic activity of the Fe_2O_3 nanocomposite samples was studied as a function of the decolorization of methylene blue (MB) dye solutions under sunlight irradiation. The photocatalytic investigation was performed during the sunny days 10 am to 4 pm at temperatures of 25°C. The experimental setting remained constant throughout the study. A 0.5g sample was dispersed into 40 mL of initial dye concentration at 5 ppm. The pH was maintained naturally, and magnetic stirring was used. To help the dye molecules stick to the photocatalyst surface better, the mixture of photocatalyst powder and solution dye was stirred for 60 minutes in the dark. During the illumination process, a 3mL volume of the MB solution was taken at regular intervals, and then the photocatalyst was manually isolated from the mixture using centrifugation. In each experiment, the equilibrium constant of the dye was determined by analyzing the sample solutions using a UV-visible spectrophotometer. This was achieved through photocatalytic degradation processes [25]. The percentage degradation of MB solution was calculated by Eq. (1) [26]:

$$\text{Degradation } \% = \frac{A_0}{A_0 - A} \times 100\% \quad (1)$$

where A_0 represents the initial absorbance, while A represents the absorbance at a specific time (t). The kinetics of photodegradation control for MB solutions can be expressed as pseudo-first-order kinetics, as in Eq. (2) [27]:

$$\text{Ln}\frac{A_0}{A} = kt \quad (2)$$

where k is the photodegradation rate constant measured in min^{-1}

3. Results and Discussion

Scanning electron microscopy (SEM) was employed to analyze the morphology of the produced samples. Figure (1a) displays the image of undoped Fe_2O_3 nanoparticles. These nanoparticles have a mostly flaky structure and are approximately 23 nm in size. Figure (1b) shows the SEM image of Fe_2O_3/Ag, in which the Fe_2O_3 nanoparticles have high homogeneity and well-defined shapes, and the particle size is 24 nm. The Fe_2O_3/Co formation is made of homogenous monodispersed, as presented in Fig. (1c), and the particle size is 31 nm. Figure (1d) shows the SEM image of the prepared Fe_2O_3/Cu sample. It is observed that as the copper gets concentrated, the particles tend to appear more clumped. Therefore, it is not possible to estimate the average particle size, whereas the particle size was approximately 20 nm. Considering Fig. (1e), the SEM images depict the aggregated structure of the Fe_2O_3/N nanocomposite, which tends to agglomerate and form larger aggregates due to its high surface energy. Agglomerates can form due to van der Waals forces and intermolecular magnetic interactions [28-29]. For this reason, the average particle size is unclear and difficult to find, and it is approximately 12 nm in size. SEM images show that Fe_2O_3/S particles, which are non-metallic and can absorb water, and their particles stick together more and more; this is illustrated in Fig. (1f), and the particle size is 26 nm.

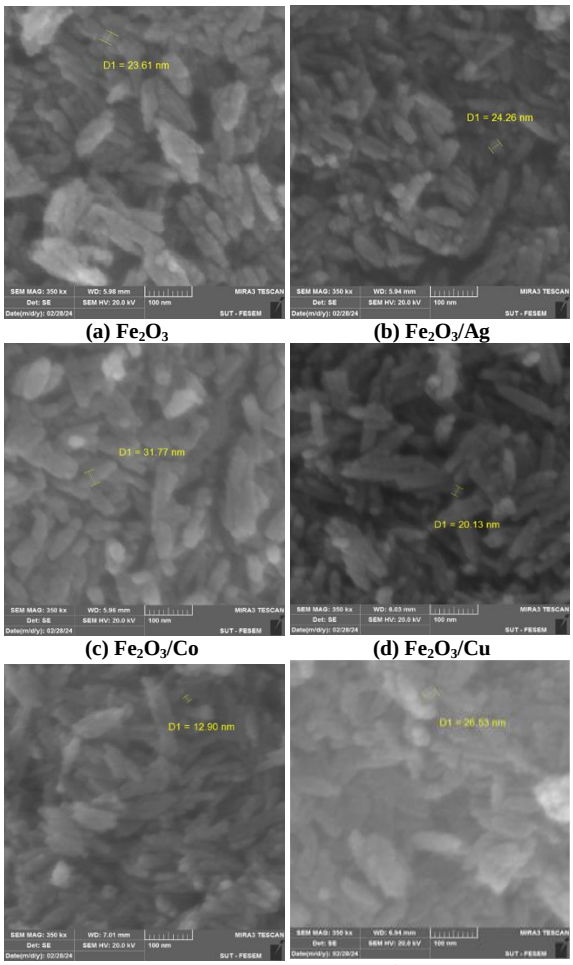

(a) Fe_2O_3 **(b) Fe_2O_3/Ag**

(c) Fe_2O_3/Co **(d) Fe_2O_3/Cu**

(e) Fe_2O_3/N **(f) Fe_2O_3/S**

Fig. (1) SEM images of (a) Fe_2O_3 (b) Fe_2O_3/Ag (c) Fe_2O_3 /Co (d) Fe_2O_3/Cu (e) Fe_2O_3/N (f) Fe_2O_3/S

Figure (2) displays the EDX spectra of metallic elements, including Fe_2O_3/Ag, Fe_2O_3/Co, and Fe_2O_3/Cu, as well as non-metallic elements Fe_2O_3/N and Fe_2O_3/S. The results indicate that the elements

Ag, Co, Cu, S, and N are spread across various energy levels. A new element, Au, has emerged among the existing elements. This element appears because its energy level is close to that of Fe_2O_3.

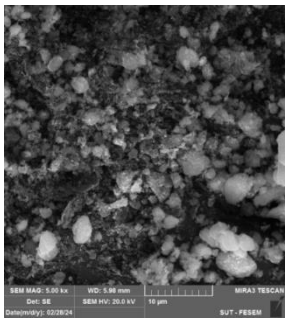

Fe_2O_3

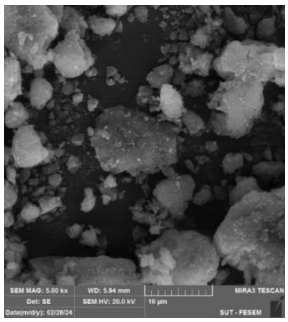

Fe_2O_3/Ag

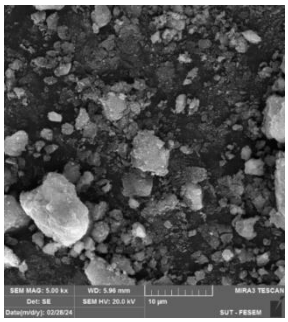

Fe_2O_3/Co

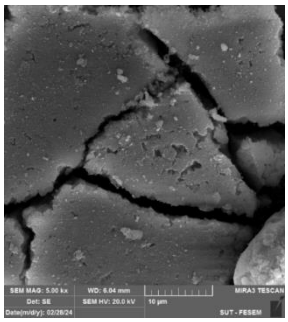

Fe_2O_3/Cu

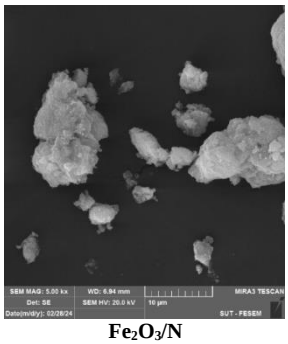

Fe_2O_3/N

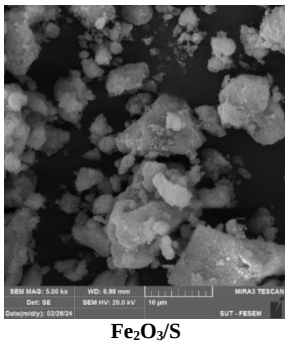

Fe_2O_3/S

(a)

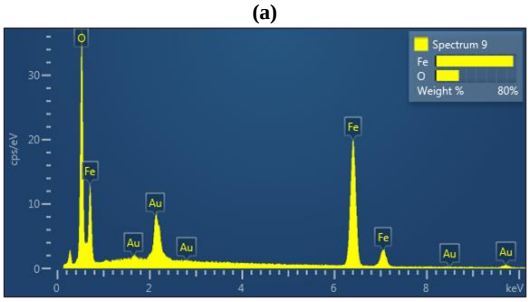

Fe_2O_3

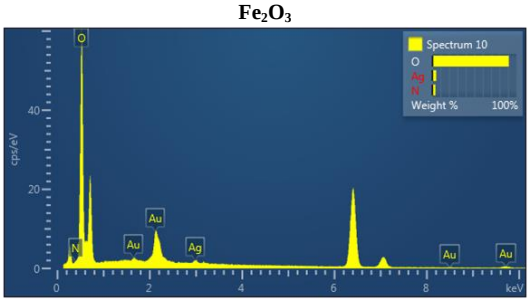

Fe_2O_3/Ag

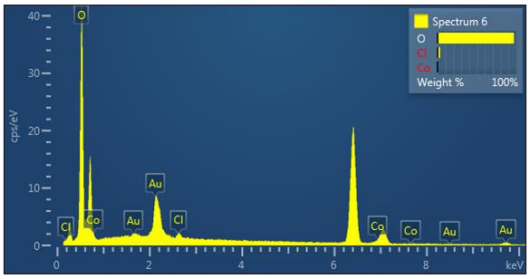

Fe_2O_3/Co

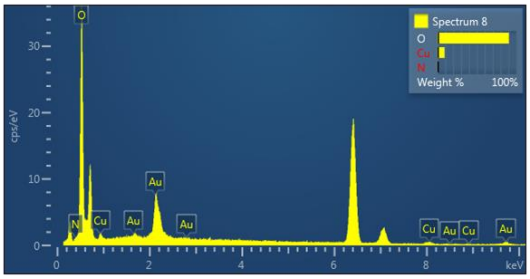

Fe_2O_3/Cu

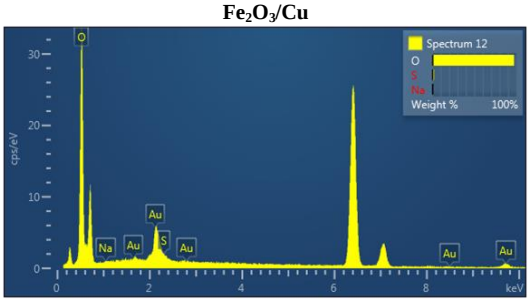

Fe_2O_3/N

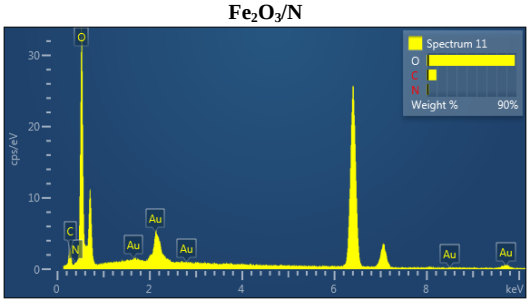

Fe_2O_3/S

(b)

Fig. (2) (a) FE-SEM and (b) EDX spectra of the samples prepared in this work

The FTIR spectroscopy is a crucial technique for detecting and analyzing the existence of functional groups and determining if there are any interactions or complexes between the components [30]. An analysis of the FTIR spectra is conducted on samples of pure Fe_2O_3, F Fe_2O_3/Ag, Co, Cu, S, and N within the frequency range of 400-4000 cm^{-1}. In case of pure Fe_2O_3 (Fig. 3a), the vibrations between 432-519 cm^{-1} indicate interactions between iron and oxygen, specifically the stretching of Fe-O bonds. Additionally, the stretching of O-H bonds around 3400 cm^{-1} shows the presence of hydroxyl groups or the absorption of water. The compound Fe_2O_3/Ag in Fig. (3b) exhibits O-H stretching and hydrogen bonding vibrations. These vibrations are characterized by peaks at 1637 cm^{-1}, which indicate the presence of amine groups, and at 1029 cm^{-1}, which indicate the presence of carboxylic acid and

ether groups. The FTIR spectra of the CO/Fe_2O_3 compound (Fig. 3c) exhibit vibrations corresponding to the Fe-O and O-Fe-O bonds. The compound Cu/Fe_2O_3 (Fig. 3d) displays absorption peaks in the 500-600 cm^{-1} range and demonstrates C=O stretching of amides at 1635 cm^{-1}. The N/Fe_2O_3 sample (Fig. 3f) exhibits O-H bond vibrations at 3281 cm^{-1} and water absorption at 1634 cm^{-1}. Additionally, Si-O vibration at 1029 cm^{-1} suggests the presence of silicon interconnections or silicates. In case of S/Fe_2O_3 (Fig. 3e), the presence of hydroxyl groups is indicated by O-H bond vibrations at 3398 cm^{-1}. Additionally, the peaks observed at 1636 and 1095 cm^{-1} show the presence of organic molecules such as lipids.

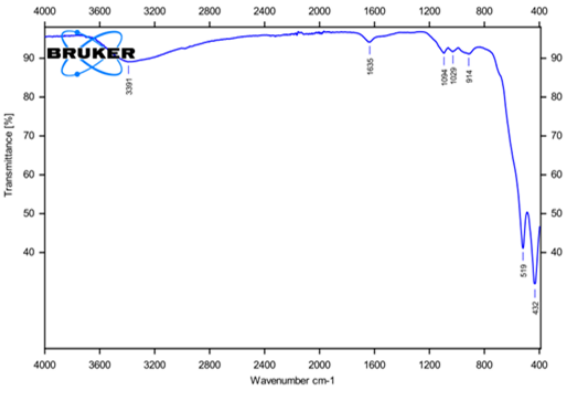

(a) Fe_2O_3

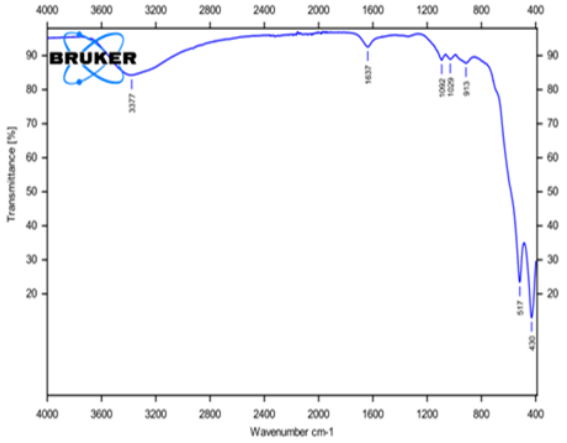

(b) Fe_2O_3/Ag

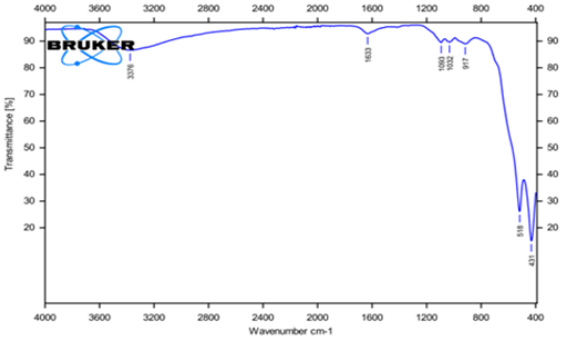

(c) Fe_2O_3/Co

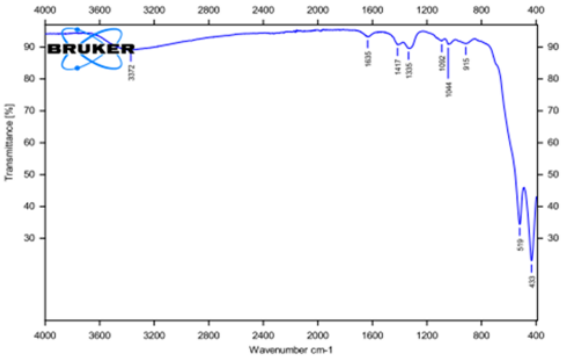

(d) Fe_2O_3/Cu

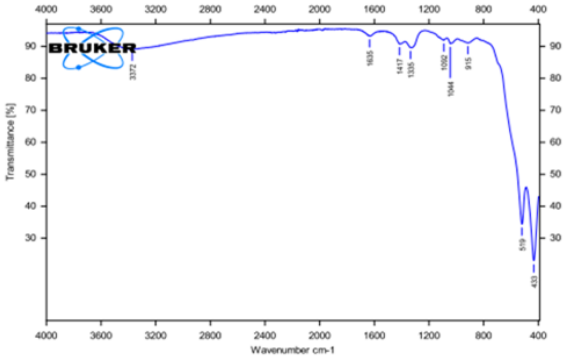

(e) Fe_2O_3/N

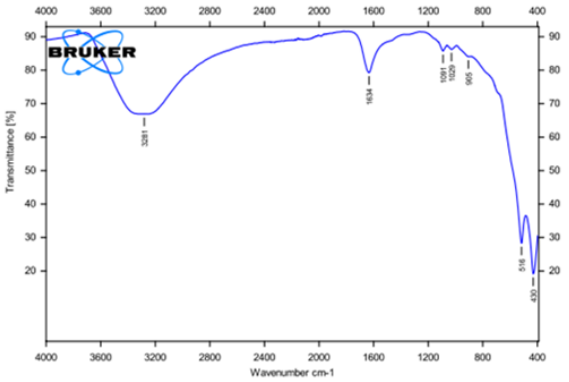

(f) Fe_2O_3/S

Fig (3) FTIR spectra of(a) Fe_2O_3 (b) Fe_2O_3/Ag (c) Fe_2O_3 /Co (d) Fe_2O_3 /Cu (e) Fe_2O_3/N (f) Fe_2O_3/S

The Fe_2O_3/Ag, Co, Cu, and Fe_2O_3/S, N nanocomposite samples were exposed to sunlight using 5 ppm from MB dye solution. MB often display a peak of absorption at 664nm in their UV-visible spectra. Figure (4) depicts that with the increase in time from 0 to 240 min., MB shows a decreased absorbance upon sunlight exposure due to photocatalytic oxidation. This is regarded as an indicator of the photocatalytic efficacy of each chemical.

Figure (5) illustrates the correlation between the breakdown of the MB solution and the concentration of Fe_2O_3 after 240 min of exposure to sunlight. (a) Fe_2O_3/Ag, Co, Cu and pure Fe_2O_3 NPs removed approximately 80%, 51%, 48% and 33% of the MB solutions, respectively. Adding silver (Ag) as a doping agent reduces the recombination on the photocatalyst surface by large margins, thus permitting holes and electrons to prevail longer and

eventually generating more hydroxyl radicals. This will increase the degradation action through sunlight exposure [31].

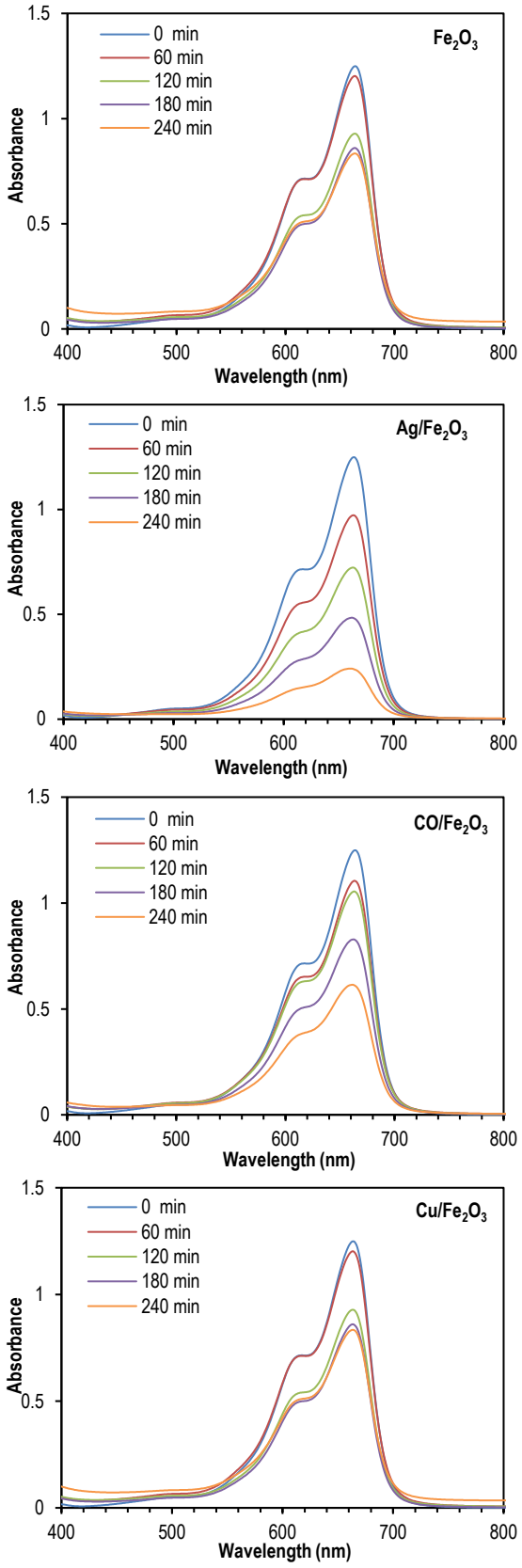

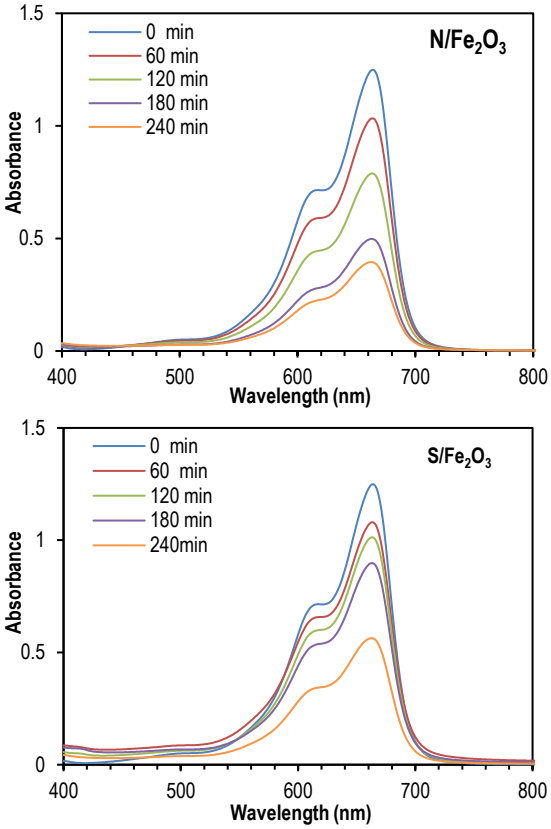

Fig (4) UV-Visible absorption spectra of Fe_2O_3, Fe_2O_3/Ag, Fe_2O_3 /Co , Fe_2O_3 /Cu , Fe_2O_3/N and Fe_2O_3/S

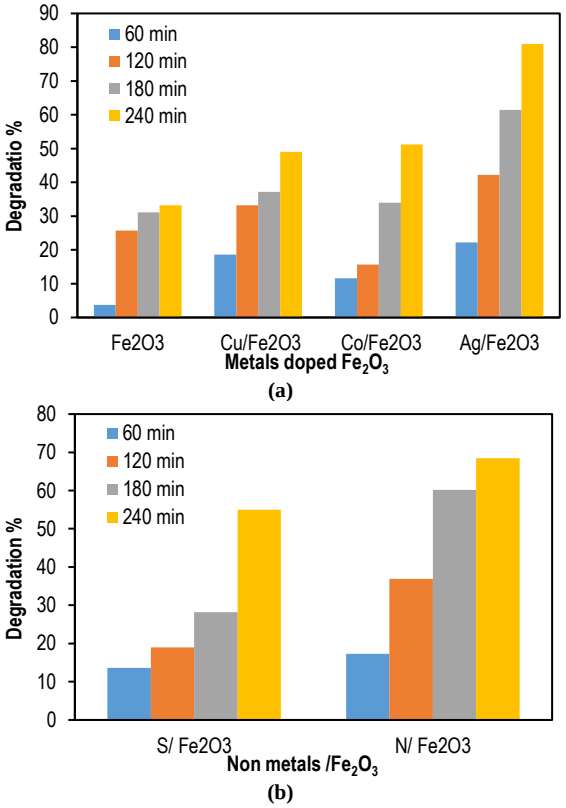

Fig. (5) MB degradation % (5ppm) by (a) Fe_2O_3, Fe_2O_3/Cu, Fe_2O_3/Co and Fe_2O_3/Ag ,(b) Fe_2O_3/N, Fe_2O_3/S under solar light irradiation

In addition, the decolorization process of Fe_2O_3, Fe_2O_3/N, and Fe_2O_3-/S was also studied. The percentages achieved after a 240min reaction period are 68% and 45%, respectively. Small-crystalline nanoparticles (N) outperform S-sized ones. This is because N nanoparticles' tiny size multiplies surface charge carrier transmission. This increases photo-induced electron-hole pair recombination, which boosts photocatalytic activity and degradation [32].

Figure (6) displays the phenomenon of decolorization in the MB solution using Fe_2O_3/Ag and Fe_2O_3/S at various degradation durations. After 120 min of sunshine exposure, the color changed from blue to light blue.

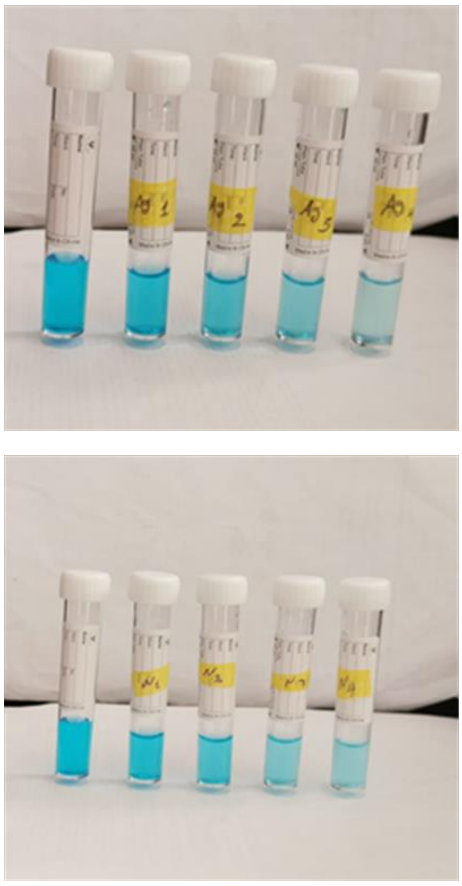

Fig. (6) MB decoloration at different photo degradation levels for Fe_2O_3/Ag and Fe_2O_3/S (5 ppm)

Figure (7) shows the correlation between the natural logarithm of absorbance (Ln A/A_0) and the duration of irradiation in minutes, offering a comparative analysis of the photocatalytic efficacy of Fe_2O_3 materials doped with various elements. The analysis emphasizes the impact of individual dopants on the rate of reaction, revealing that Ag/Fe_2O_3 and N/Fe_2O_3 had the most pronounced photocatalytic activity, whereas the remaining materials have shown comparatively lower efficacy plots according to Eq. (2).

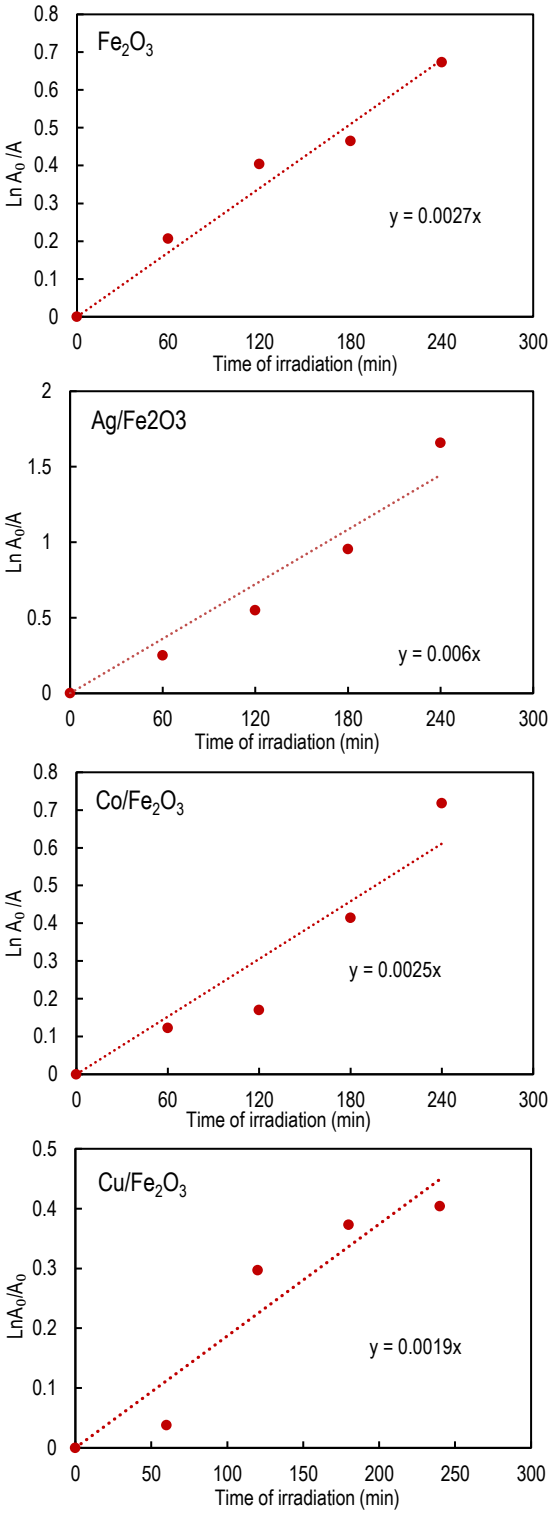

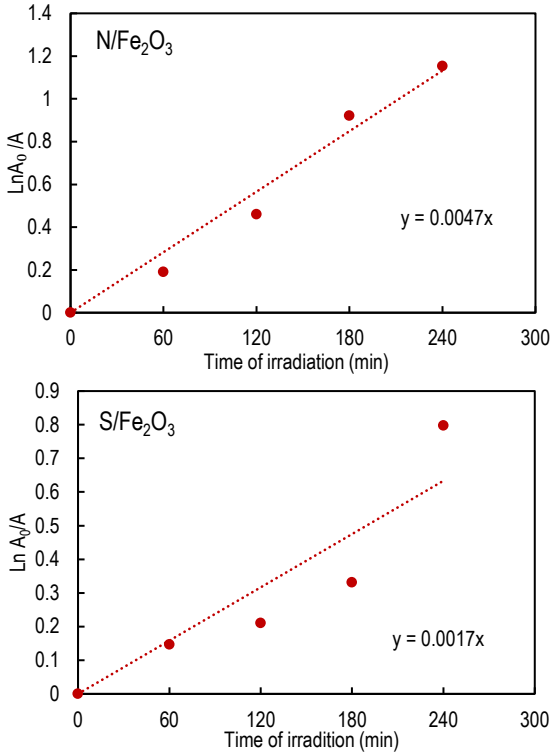

Fig. (7) Ln (A_o/A) vs. reaction time t of MB (5 ppm) decomposition catalyzed by metal Fe_2O_3/Ag, Co, Cu and nonmetal Fe_2O_3/S, N under sunlight irradiation

According to the data in table (1), the rate constants (k) can be determined by analyzing the slope of linear plots that depict the relationship between ln(A/A_0) and time. The optimal sample of Fe_2O_3/Ag shows k value of 0.006 min^{-1}.

Table (1) Different Fe_2O_3/Ag, Co, Cu, N, S degradation rate constants (5 ppm)

Samples	Rate constant (k) min^{-1}
Fe_2O_3	0.0019
Fe_2O_3/Ag	0.006
Fe_2O_3/Co	0.0025
Fe_2O_3/Cu	0.0027
Fe_2O_3/N	0.0047
Fe_2O_3/S	0.0017

4. Conclusion

In concluding remarks, the grafting of metal ions (Ag, Co, Cu) and nonmetal ions (N, S) onto iron oxide nanoparticles (Fe_2O_3) significantly affects the photocatalytic performance. A simple impregnation method was used for successful incorporation of the dopants to improve light absorption efficiency, enhance charge separation, and reduce recombination rates, leading to better photocatalytic activity. The results indicate that Ag ions are the optimum doping material to achieve the best photocatalytic activity of Fe_3O_4 nanoparticles as they resulted in increase in degradation of the MB dye by 80% under sunlight.

References

[1] A.S. Khalil, B.M. Al-Shabander and H.M. Yaseen, "Photocatalytic activity of tetragonal $BaTiO_3$ nanoparticles prepared by wet chemical method", *AIP Conf. Proc.*, 2372(1) (2021) 130019.

[2] K.R. et al., "Exploring the effect of crystalline phase on photocatalytic, antimicrobial and antioxidant performance of magnetic iron oxide nanoparticles", *Nano Struct. Nano Obj.*, 38 (2024) 101166.

[3] M.B. Al-Taee and B.M. Alshabandar, "Photocatalytic degradation of methyl blue by TiO_2 nanoparticles incorporated in cement", *Iraqi J. Phys.*, 21(1) (2023) 10-20.

[4] A.T. Bell, "The impact of nanoscience on heterogeneous catalysis", *Science*, 299(5613) (2003) 1688-1691.

[5] D. Friedmann et al., "Heterogeneous photocatalytic organic synthesis: state-of-the-art and future perspectives", *Green Chem.*, 18(20) (2016) 5391-5411.

[6] V. Augugliaro et al., "Overview on oxidation mechanisms of organic compounds by TiO_2 in heterogeneous photocatalysis", *J. Photochem. Photobiol. C: Photochem. Rev.*, 13(3) (2012) 224-245.

[7] A.A. Almarasy, S.A. Azim and E.M. Ebeid, "The application of hematite (α-Fe_2O_3) nanoparticles in coagulation and flocculation processes of River Nile Rosetta branch surface water", *SN Appl. Sci.*, 1 (2019) 1-6.

[8] K. Sivula, F. Le Formal and M. Grätzel, "Solar water splitting: progress using hematite (α-Fe_2O_3) photoelectrodes", *Chem. Sust. Chem.*, 4(4) (2011) 432-449.

[9] C. Wu et al., "Synthesis of hematite (α-Fe_2O_3) nanorods: diameter-size and shape effects on their applications in magnetism, lithium ion battery, and gas sensors", *The J. Phys. Chem. B*, 110(36) (2006) 17806-17812.

[10] D.W. Elliott and W.-X. Zhang, "Field assessment of nanoscale bimetallic particles for groundwater treatment", *Enviro. Sci. Technol.*, 35(24) (2001) 4922-4926.

[11] S. Giri et al., "Magnetic properties of α-Fe_2O_3 nanoparticle synthesized by a new hydrothermal method", *J. Magnet. Magnet. Mater.*, 285(1-2) (2005) 296-302.

[12] S. Mornet et al., "Magnetic nanoparticle design for medical applications", *Prog. Solid State Chem.*, 34(2-4) (2006) 237-247.

[13] S.A. Al-Lhaibi and B.M. Al-Shabander, "Photocatalytic Activity and Wettability Properties of ZnO/Sawdust/Epoxy Composites", *Iraqi J. Phys.*, 20(4) (2022) 54-65.

[14] H.A. Alrubaie and B.M. Muzahem, "Variation of pH and composite dosage on the photocatalytic activity for ZnO/epoxy nanocomposites", *Iraqi J. Phys.*, 19(51) (2021) 33-40.

[15] S. Hmamouchi, A. El Yacoubi and B.C. El Idrissi, "Using egg ovalbumin to synthesize pure α-Fe_2O_3 and cobalt doped α-Fe_2O_3: structural,

morphological, optical and photocatalytic properties", *Heliyon*, 8(2) (2022).
[16] B.J. Rani et al., "Sn doped α-Fe_2O_3 (Sn= 0, 10, 20, 30 wt.%) photoanodes for photoelectrochemical water splitting applications", *Renew. Ener.*, 133 (2019) 566-574.
[17] O. Koplak et al., "Effect of α-Fe_2O_3 microbeads on CoFeB/Ta/CoFeB magnetic switching and magnetic instabilities", *Superlat. Microstruct.*, 121 (2018) 23-32.
[18] A.S. Khalil, "Photocatalytic characterization of TiO_2 nanorods and nanotubes synthesized by sol gel template method", *Eng. Technol. J.*, 36(2) (Part C) (2018).
[19] B.M. Al-Shabander and E.A. AL-Ajaj, "Study the photocatalytic behavior of TiO_2 nanoparticles doped with Ni synthesized by sol-gel method", *Int. J. Appl. Innov. Eng. Manag.*, 5(2) (2016) 37-42.
[20] B.M. Alshabandar, "Copper (II)-doped WO_3 nanoparticles with visible light photocatalytic antibacterial activity against gram-positive and gram-negative bacteria", *Inorg. Nano-Metal Chem.*, 50(12) (2020) 1329-1333.
[21] A. Lassoued et al., "Synthesis, structural, morphological, optical and magnetic characterization of iron oxide (α-Fe_2O_3) nanoparticles by precipitation method: effect of varying the nature of precursor", *Physica E: Low-dim. Syst. Nanostruct.*, 97 (2018) 328-334.
[22] K. Supattarasakda et al., "Control of hematite nanoparticle size and shape by the chemical precipitation method", *Powder Technol.*, 249 (2013) 353-359.
[23] B.T. Hang and D.H. Thang, "Electrochemical properties of Fe_2O_3 microparticles and their application in Fe/air battery anodes", *J. Alloys Comp.*, 655 (2016) 44-49.
[24] N.V. Long et al., "Controlled synthesis and characterization of iron oxide micro-particles for Fe-air battery electrode material", *Colloid Polym. Sci.*, 293 (2015) 49-63.
[25] H.A. Alrubaie and B.M. Alshabander, "The effect of ZnO nanoparticles on the self-cleaning of ZnO/epoxy composites", *AIP Conf. Proc.*, 2437(1) (2022).
[26] J. Strunk (ed.), **"Heterogeneous Photocatalysis: From Fundamentals to Applications in Energy Conversion and Depollution"**, John Wiley & Sons (2021).
[27] J.C. Colmenares and Y.-J. Xu, "Heterogeneous photocatalysis, From Fundamentals to Green Applications", Springer (2016).
[28] M. Ozaki et al., "Agglomeration in colloidal hematite dispersions due to weak magnetic interactions: II. The effects of particle size and shape", *J. Colloid Interface Sci.*, 126(1) (1988) 212-219.
[29] R. Kant, D. Kumar and V. Dutta, "High coercivity α-Fe_2O_3 nanoparticles prepared by continuous spray pyrolysis", *RSC Adv.*, 5(65) (2015) 52945-52951.
[30] W. Demtröder, **"Atoms, Molecules and Photons"**, Springer (2010).
[31] H.-M. Lo et al., "Improving the efficiency of metal ions doped Fe_2O_3 nanoparticles: photocatalyst for removal of organic dye from aqueous media", *Chemosphere*, 337 (2023) 139229.
[32] B.M. Al-Shabander and E.A. Ajaj, "Urea modified TiO_2 nanoparticles prepared by Sol-Gel method to enhance the photocatalytic activity under sunlight", *Eng. Technol. J.*, 33(9) (Part B) (2015).

